Int. J. Heat Mass Transfer. Vol. 36, No. 10, pp. 2665–2674, 1993
Printed in Great Britain

0017-9310/93 $6.00+0.00

Near-field solution for heat and mass transfer from buried nuclear waste canisters

K. MURALIDHAR
Department of Mechanical Engineering, Indian Institute of Technology, Kanpur—208016, India

(*Received* 11 *May* 1992)

Abstract—A numerical study of heat and mass transfer from cylindrical containers filled with nuclear waste and buried under the surface of the earth is reported here. For prescribed heat flux and leach rates the temperature and concentration distributions on the surface of the containers are determined under a variety of conditions. These conditions include the diffusion limit, the effect of superimposed flow, the multi-canister problem and radioactive decay of a parent–daughter chain. The equations governing unsteady transport are solved using a Galerkin finite element method. Results computed using this method are compared with those obtained from boundary-layer analysis.

INTRODUCTION

DISPOSAL of radioactive waste in cylindrical containers under the surface of the earth has gained wide acceptance in the nuclear power industry. To carry out a safety analysis and gauge the impact of this practice on the environment it is necessary to determine flow patterns and heat and mass transfer rates in the vicinity of these containers. The present work is a numerical study of this problem and a variety of controlling factors have been taken into account. The waste canisters are assumed to be buried in a water-saturated, homogeneous, isotropic porous medium. A canister would release thermal energy at its surface owing to the decay of radioactive waste contained within it. Mass transfer occurs at the surface of the canister due to leaching by the groundwater. The important questions to be answered are, (1) the maximum temperature and concentration levels attained in the flow domain and (2) the size of the region affected by the canister. Maximum temperature and concentration levels invariably occur on the surface of the canisters themselves. On the other hand safety analysis is usually performed over a long time period and the size of the affected region is large in comparison to the canister diameter. Hence the two questions given above address problems with length scales that differ by several orders of magnitude.

The far field problem has been addressed quite extensively in the literature; for example see Broyd [1], Huyakorn *et al.* [2]. When the domain size under consideration is large it is important to include heterogeneity and anisotropy of the porous formation and adsorption–desorption effects in heat and mass transfer. These effects are not significant in the near field problem and the assumption of a homogeneous and isotropic porous medium is adequate. However, the near-field solution must include the canister geometry, interaction effects between them, distortion to the flow path and appropriate boundary conditions for heat and mass transfer on the canister surface.

Kimura [3, 4] has numerically studied transient and steady state heat transfer from a canister buried in a porous medium under conditions of cross-flow and parallel flow. Kimura's work assumes that the surface of the canister is at a uniform temperature. In the present study we assume that the heat flux is prescribed at the canister surface and the temperature level adjusts itself according to flow conditions prevailing in the porous region. We consider canisters and canister arrays under forced flow conditions in which variable density effects are ignored. The flow is assumed to occur normal to the axis of the cylinder. The equations governing heat and mass transfer in the presence of flow are solved using a Galerkin finite element method. The predictions of the numerical scheme are compared with those obtained from boundary-layer analysis of the heat and mass transfer problems. Both transient and steady state analyses have been included in the study. The emphasis in the present work is obtaining temperature and concentration levels on the canister surface when the heat and mass flux rates are prescribed subject to a variety of external factors. These factors are, the diffusion limit, inter-canister interaction due to proximity, effect of fluid flow, radioactivity decay and nuclide chain consisting of a parent and a daughter.

Several important decay reactions that are relevant to near and deep surface burial of nuclear waste can be represented as a parent–daughter model. Here the parent has a finite half life and the daughter is long-lived or stable. Intermediate nuclides may be formed but are sufficiently short-lived to be ignored. The model that we consider for these reactions is $A \rightarrow B$ with decay constants λ_A and λ_B. Here λ, the decay constant ($=0.693/\text{half-life}$), is zero for a stable element.

In solving a mass transfer problem for a parent and a daughter nuclide their respective transport prop-

NOMENCLATURE

b	decay parameter
b_A, b_B	decay parameter of nuclides A and B
c	concentration
c_A, c_B	concentration of nuclides A and B
D	dispersion coefficient
J, Y	Bessel functions of the first and second kind
K	local permeability
N	norm in equation (12)
Pe	Peclet number
r	radial coordinate
R	radius of canister
R_0	eigenfunction in equation (12)
R_p	fraction of parent nuclide converted into the daughter
T	temperature
$\mathbf{u}$	velocity vector
x, y	Cartesian coordinates.

Greek symbols

β	parameter in Fourier transform, also retardation factor
δ	boundary-layer thickness
θ	angular coordinate
λ	decay constant
Ψ	stream function.

Other symbols

∇	gradient operator $[(\partial/\partial x), (\partial/\partial y)]$
c_t, c_x	$(\partial c/\partial t)$, $(\partial c/\partial x)$.

erties and leach rates from the canister surface must be specified. It is assumed here that the parent and daughter nuclides being close to each other in the periodic table will have similar transport properties. Further the leach rates are assumed to be either identical or that for the daughter is taken to be zero.

FORMULATION

Convective heat and mass transfer is governed by an equation of the form (Kays and Crawford [5]),

$$c_t + \mathbf{u}\cdot\nabla c = D\nabla^2 c - \lambda c + R_p\lambda_p c_p \qquad (1)$$

c represents temperature in heat transfer problems and concentration of a nuclide in mass transfer problems. Equation (1) must be solved subject to a cold or a clean initial state, $t = 0$, $c = 0$ and prescribed flux on the canister surface, $-(\partial c/\partial n) = q$. c is taken to be zero in the flow approaching the canisters. The flow configuration is shown in Fig. 1. Here n is an outward drawn normal on the canister surface and q is the heat flux in heat transfer and leach rate in mass transfer problems. q is taken to be a prescribed constant in the present work. In equation (1) D is a dispersion coefficient, λ is the decay constant, λ_p is the decay constant of the parent nuclide, R_p is the fraction of the parent nuclide converted into the nuclide under study and c_p is the parent concentration. In general c_p must be determined from another equation similar to equation (1). A variety of special cases arise from the general mass transfer problem represented by equation 1. These are discussed below.

Non-dimensionalization. Using a velocity U that prevails in the undisturbed part of the flow domain as a velocity scale and the canister radius R as the length scale the convective mass transfer problem is written in dimensionless form as follows:

$$c_t + \mathbf{u}\cdot\nabla c = \frac{1}{Pe}\nabla^2 c - bc + R_p b_p c_p \qquad (2)$$

with the initial and boundary conditions, $c(t = 0) = 0$, $-(\partial c/\partial r)(r = 1) = 1$ and $c(r = \infty) = 0$.

In equation (2) r is a radial coordinate measured from the centre of the canister. c is scaled by qR, b is $\lambda R/U$ and Pe, the Peclet number is UR/D. The characteristic time scale is R/U. For the special case of $U = 0$ the diffusion limit, the velocity scale is chosen as D/R and so the scales for λ and t are D/R^2 and R^2/D respectively.

The diffusion limit for a single nuclide (i.e. $R_p = 0$) is reached in equation (3) by setting $\mathbf{u} = 0$, using D/R as the velocity scale and R^2/D as the time scale. This yields

$$c_t = \nabla^2 c - bc \qquad (3)$$

with initial and boundary conditions as in equation (2). Here b is defined as $\lambda R^2/D$ and

$$\nabla^2 = \left(\frac{\partial^2}{\partial r^2} + \frac{1}{r}\frac{\partial}{\partial r} + \frac{1}{r^2}\frac{\partial^2}{\partial\theta^2}\right).$$

The equations governing unsteady transport of a parent and a daughter nuclide, to be called A and B respectively and undergoing a reaction A → B are as follows:

$$\underline{\text{A}} \qquad c_t + \mathbf{u}\cdot\nabla c = \frac{1}{Pe}\nabla^2 c - b_A c$$

$$\underline{\text{B}} \qquad c_t + \mathbf{u}\cdot\nabla c = \frac{1}{Pe}\nabla^2 c - b_B c + b_A c_A. \qquad (4)$$

Equations (4) are obtained from equation (2) by setting $R_p = 0$ and 1, respectively.

The following boundary conditions have been considered in the present study.

Equal leach rates of A and B:

$$-\frac{\partial c_A}{\partial r} = -\frac{\partial c_B}{\partial r} = 1.$$

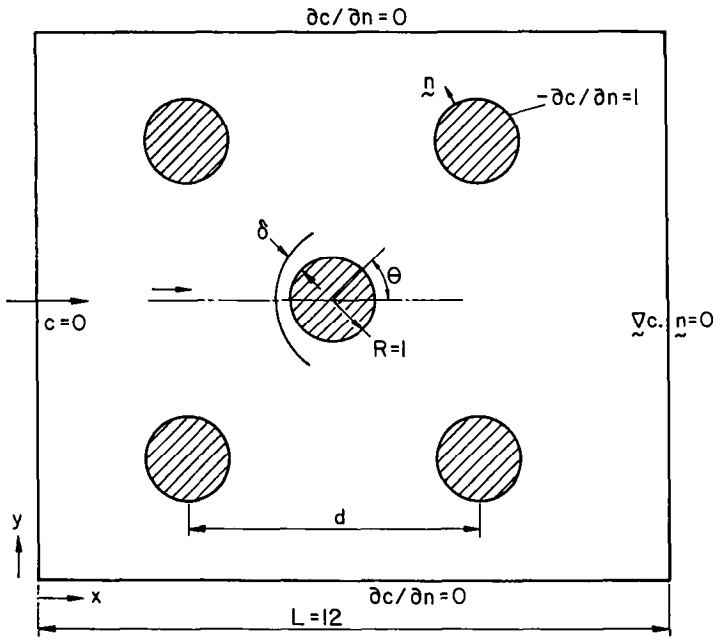

FIG. 1. Canister layout and coordinate system.

Unequal leach rates of A and B:

$$-\frac{\partial c_A}{\partial r} = 1, \quad -\frac{\partial c_B}{\partial r} = 0.$$

The second boundary condition models the problem where the daughter nuclide is entirely produced by decay of the parent in the flow. In equation (4) the Peclet number is defined as $Pe = UR/D$, where D, the dispersion coefficient, is assumed to be identical for A and B.

Equation (2) also represents mass transfer with adsorption if the adsorption reaction can be represented as a linear isotherm (Bear [6]). In this case the characteristic scale for time is $\beta R/U$ and the decay parameter b is $\beta R/U$. $\beta \geqslant 1$ is the retardation factor of the nuclide under study.

Heat transfer. Setting $\lambda = 0$ and replacing c by T gives us the equation governing heat transfer namely,

$$T_t + \mathbf{u}\cdot\nabla T = \frac{1}{Pe}\nabla^2 T$$

with

$$T(t=0) = 0, \quad -\frac{\partial T}{\partial r}(r=1) = 1$$

and

$$T(r=\infty) = 0. \tag{5}$$

At steady state T_t is set equal to zero in equation (5). At the diffusion limit $u = 0$ and using appropriate scales equation (4) reduces to,

$$T_t = \nabla^2 T \tag{6}$$

with initial boundary conditions as given in equation (5).

It is worth noting that equations (1)–(5) admit a steady state solution but none exists for equation (6). This can be traced to the fact that competing mechanisms of production, decay and transport of mass or energy exist in the former but not at the pure diffusion limit. In a pure diffusion problem the surface temperature of the canister increases without limit with time. In practice increasing temperature beyond a certain limit will lead to buoyancy-driven convection around the canister and force a steady state to be attained.

The multicanister problem is treated by solving equations (1)–(6) with the boundary condition $-c_r = 1$ applied on each canister surface. At the diffusion limit the governing equations are linear and the concentration at a point is obtained by linear superposing the individual effects of canisters around it. In the presence of flow the velocity vector $\mathbf{u}$ is altered because of obstructions in the flow path and $\mathbf{u}$ changes with number and pattern of distribution of the canisters. Hence the method of superposition is not applicable here.

Determination of the velocity field

Flow in a saturated, homogeneous, isotropic porous medium is assumed to be governed by Darcy's law,

$$\mathbf{u} = -\frac{K}{\mu}\nabla p,$$

the incompressibility constraint $\nabla\cdot\mathbf{u} = 0$ and the

boundary condition $\mathbf{u}\cdot\mathbf{n}=0$ on impermeable surfaces. For flow past a single cylinder these equations can be solved using potential theory. This yields,

$$u-\mathrm{i}v=1-\frac{1}{z^2} \quad \text{where} \quad z=x+\mathrm{i}y, \quad \mathrm{i}=\sqrt{(-1)}$$

and u and v are Cartesian components of velocity. For flow past an array of cylinders the permeability K appearing in Darcy's law is made a spatial variable with a value of unity in the porous region and a small value, around 10^{-7} over the area occupied by the cylinder. The velocity problem is then solved numerically in terms of a stream function Ψ which is related to velocity as $\mathbf{u}=(\Psi_y, -\Psi_x)$. The equation governing Ψ can be shown to be,

$$\nabla\cdot\frac{1}{K}\nabla\Psi=0 \tag{7}$$

with the approach flow condition $(\Psi_y, -\Psi_x)=(1,0)$ i.e. $\Psi=y$ ahead of the cylinder array.

In the present study calculations have been carried out on a square domain in which a single cylinder or any array of cylinders is present. This is shown in Fig. 1. With reference to this figure the boundary conditions for equation (7) are,

$$x=0 \quad \Psi=y;\ y=0 \quad \Psi=0;\ y=L \quad \Psi=L$$
$$\text{and} \quad x=L \quad \Psi_x=0.$$

The size of the region L in relation to the cylinder radius has been chosen to be 12 units in the present work. Equation (7) has been solved by a control volume finite difference method with harmonic averaging for K at the interface between the cylinder and the porous region. A grid size of 201×201 has been found to be adequate to obtain grid-independent velocity profiles. The agreement between the velocity fields computed analytically and from equation (7) for a single cylinder is found to be excellent.

Finite element solution. Steady and unsteady convective heat and mass transfer from single canisters and canister arrays have been studied in this work using a Galerkin finite element method (Baker [7]). Six-noded isoparametric triangular elements have been used for interpolation of the temperature and concentration fields. Implicit finite differencing is used to march in time. Matrix inversion is accomplished using a sparse matrix solver (Duff [8]). The grid that is used discretizes each canister surface with 16 nodes. Grid smoothness is guaranteed by the use of a Laplace equation for grid generation. Equation (2) is known to become computationally intractable for large values of the convection parameter Pe. In the present work the grid used is found to be adequate for values of Pe up to 50. Higher values of Pe lead to oscillations in the temperature and concentration fields that can be resolved only by grid refinement. In the nuclear waste disposal problem studied here values of Pe greater than 50 are not expected both because the velocity U is small and the dispersion coefficient D is large. For typical values of $U=10$ m yr^{-1}, $R=1$ m and $D=10$ m^2 yr^{-1} Pe is unity. The testing of the finite element code for solving convective heat transfer problems is described in the author's work reported elsewhere (Muralidhar [9]). Further comparison with a boundary-layer solution for flow past a single cylinder is reported later in this study.

Finite element calculations have been carried out on a domain of size of 12×12 units and a canister radius of unity. The coordinate system used and the boundary conditions on various sides of the flow domain are shown in Fig. 1. In unsteady problems a variable time step is used. The time steps used in the present study are $\Delta t=0.01$ for $t<0.1$ and $\Delta t=0.1$ for $t>0.1$.

Boundary-layer solution. Steady flow past a single cylinder at high Peclet numbers ($Pe>1$) will lead to the formation of a boundary-layer on its surface. This is shown in Fig. 1. All changes in c and T are confined to the region $1<r<1+\delta$ and each is zero outside this region. The boundary-layer thickness grows on the cylinder surface and is a function of θ. If the boundary-layer is thin i.e. $\delta/R\ll 1$, where δ is the thermal or concentration boundary-layer thickness, the governing equation for c or T can be simplified. If $\delta/R\ll 1$ the derivatives parallel to the cylinder wall are small in comparison to those normal to it, i.e. $\partial/\partial\theta\ll\partial/\partial r$ and $\partial^2/\partial\theta^2\ll\partial^2/\partial r^2$ and equation (2) reduces to,

$$(uc)_\theta=\frac{1}{Pe}(rc_r)_r-rbc+rb_pR_pc_p \tag{8}$$

where r and θ are polar coordinates measured from the centre of the cylinder and u is now the tangential component of velocity. From potential theory the tangential component of velocity on the canister surface is, $u=-2\sin\theta$ for flow past a single cylinder buried in a porous medium. Equation (8) is solved by first assuming a profile for c in terms of r with δ as a parameter. δ is then determined from an integrated form of equation (8).

The form for c assumed in the present work is,

$$c=\frac{\delta}{2}\left(1-\left(\frac{r-1}{\delta}\right)\right)^2.$$

It satisfies the boundary conditions $r=1$, $-c_r=1$ and $r=1+\delta$, $c=0$ automatically. The value of c at the canister surface is $\delta/2$. The equation governing δ is obtained by integrating equation (8) as $\int_1^{1+\delta}\mathrm{d}r$. For a single nuclide problem ($R_p=0$) this results in the following first order ordinary differential equation.

$$\frac{\mathrm{d}\phi}{\mathrm{d}\theta}+\left\{\left(\cot\theta-\frac{b}{2}\operatorname{cosec}\theta\right)\phi-\frac{b}{8}\operatorname{cosec}\theta\phi^{3/2}\right\}=-\frac{3\operatorname{cosec}\theta}{Pe}. \tag{9}$$

Here $\phi=\delta^2$. The initial condition for ϕ is obtained

from equation (9) by setting $d\phi/d\theta = 0$ as $\theta \to \pi$. Hence,

$$\theta = \pi, \quad \left(1+\frac{b}{2}\right)\phi + \frac{b}{8}\phi^{3/2} = \frac{3}{Pe}. \tag{9a}$$

$\phi(\pi)$ is obtained as the algebraic root of equation (9a), by a Newton–Raphson scheme. Equation (9) is integrated by a fourth order Runge–Kutta scheme. The heat transfer problem is recovered from equations (9) and (9a) by setting the decay parameter $b = 0$. For large values of b and Pe equation (9) becomes stiff. In the present work the flow domain $0 < \theta < \pi$ has been covered by 2400 steps and all computations employ double precision arithmetic. Equation (9) exhibits singularity at $\theta = 0$ and δ and c are unbounded at this location. This singularity is related to the boundary-layer model for heat and mass transfer and is not observed in the finite element simulations. In computing the average temperature and concentration of a cylinder using equation (9) the value $\delta(0)$ is ignored. However the increase in the magnitude δ as $\theta \to 0$ consistently over-predicts the average values of c and T with respect to the finite element solution.

For a pair of elements A and B that react A → B, where A is the parent and B is the daughter nuclide the boundary-layer equations are given below.

Parent

$$\frac{d\phi_A}{d\theta} + \left\{\left(\cot\theta - \frac{b_A}{2}\operatorname{cosec}\theta\right)\phi_A - \frac{b_A}{8}\operatorname{cosec}\theta\,\phi_A^{3/2}\right\} = -\frac{3\operatorname{cosec}\theta}{Pe} \tag{10}$$

$$\theta = \pi, \quad \left(1+\frac{b_A}{2}\right)\phi_A + \frac{b_A}{8}\phi_A^{3/2} = \frac{3}{Pe}$$

Daughter

$$\frac{d\phi_B}{d\theta} + \left\{\left(\cot\theta - \frac{b_B}{2}\operatorname{cosec}\theta\right)\phi_B - \frac{b_B}{8}\operatorname{cosec}\theta\,\phi_B^{3/2}\right\} = -\operatorname{cosec}\theta\left(\frac{3}{Pe} + \frac{b_A}{2}\left(\phi_A + \frac{\phi_A^{3/2}}{4}\right)\right) \tag{11}$$

$$\theta = \pi, \left(1+\frac{b_B}{2}\right)\phi_B + \frac{b_B}{8}\phi_B^{3/2} = \frac{3}{Pe} + \frac{b_A}{2}\left(\phi_A + \frac{\phi_A^{3/2}}{4}\right).$$

Here ϕ_A and ϕ_B are δ_A^2 and δ_B^2 respectively. b_A and b_B are the decay parameters of nuclides A and B respectively.

RESULTS

The temperature and concentration levels prevailing on the surface of single canisters and those placed in an array are presented here. Various factors that influence these levels are separately considered.

Diffusion limit

For a single canister the concentration field is axisymmetric in the absence of a superimposed flow, i.e. $\partial/\partial\theta = 0$. The solution of equation (3) subject to the gradient condition $-c_r|_{r=1} = 1$ can be obtained by Fourier transforms. It is given as,

$$c(r,t) = \int_0^\infty \frac{\beta R_0(\beta,r)R_0(\beta,1)}{N(\beta)(\beta^2+b)}\left(1-e^{-(\beta^2+b)t}\right)d\beta \tag{12}$$

where

$$R_0(\beta,r) = J_0(\beta r)Y_1(\beta) - Y_0(\beta r)J_1(\beta)$$

and

$$N(\beta) = J_1^2(\beta) + Y_1^2(\beta).$$

J and Y are Bessel functions of the first and second kind and their order is represented by their subscript. The integral given above converges as $t \to \infty$ only if $b > 0$. Hence a steady state solution for c does not exist for the heat transfer problem. The value of $c(1,t)$ has been numerically evaluated in the present work using Simpson's rule. A value of $\beta = 100$ for the upper limit of integration and 8001 points for Simpson's rule to produce converged results for c. Such a large number of integration points is required in particular for small values of b and large time.

The variation of the wall concentration $c(1,t)$ with time and with b as a parameter is shown in Fig. 2. It is seen that c increases without limit when $b = 0$ but a steady state is attained for finite values of b. Steady state is attained faster at higher values of b. Under these conditions the amount of c produced at the surface of the canister is annihilated by decay of the nuclide in the region surrounding the canister. For a canister radius $R = 1$ m, $D = 1.0$ m^2 yr^{-1} and a half-life of 100 yr $b = R^2\lambda/D$ can be calculated as 0.69×10^{-2}. For long-lived isotopes b is much smaller and the solution for $b = 0$ must be used.

Diffusive heat and mass transfer from a canister placed in a symmetric array with a spacing 'd' (Fig. 1) is considered next. The concentration on the central canister can be expected to be larger than the values of c on the remaining four canisters since the latter are exposed to an unbounded region on a portion of their surface. The value of $c(1,t)$ on the central canister is obtained by computing the effect of each canister individually using equation (12) and summing up these values. For an array the concentration distribution is no longer axisymmetric. However direct calculations of c on the central canister show c to be only a weak function of θ with the maximum and minimum values being within 2% of each other. The values given below are the maximum values of $c(1,t)$ on the central canister. For the array pattern considered in Fig. 1 these occur at $\theta = 0$, $\pi/4$ and $\pi/2$ in each quadrant.

Figure 3 shows the effect of the canister spacing d on the transient growth of $c(1,t)$ on the central canister. The effect of the neighbouring canisters is seen to

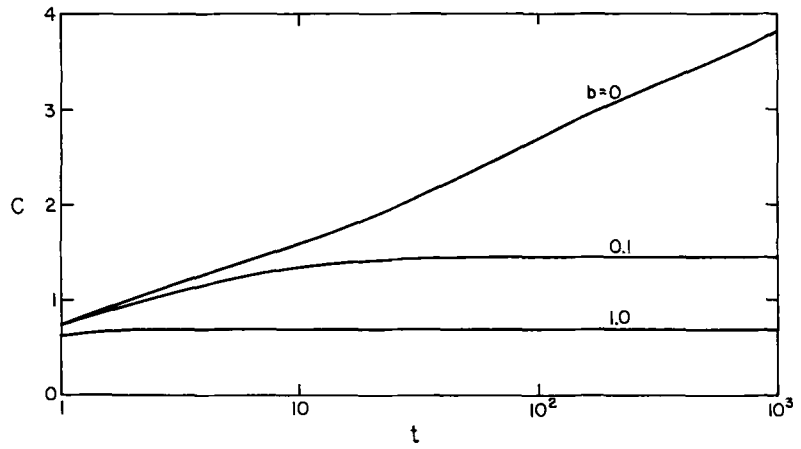

FIG. 2. Increase in wall concentration with time: diffusion limit.

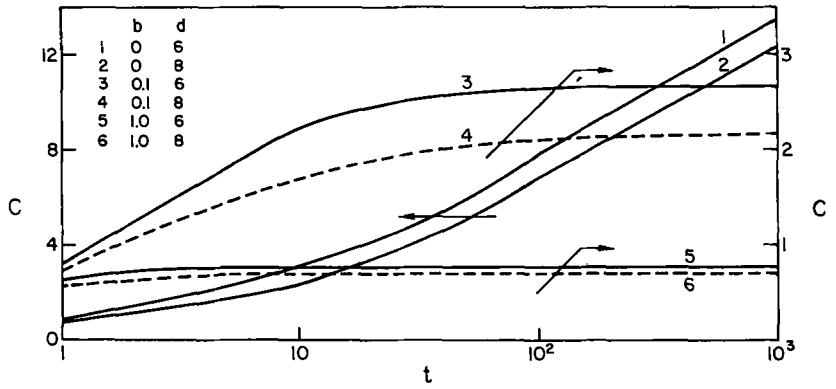

FIG. 3. Increase in wall concentration of the central canister in an array: diffusion limit.

be most pronounced at large time, small d and small values of b. Under these conditions the region around the canister that is affected by heat and mass transfer at its surface is large resulting in interference effects between canisters.

Flow past canisters: Steady state

Steady heat and mass transfer from canisters placed in a prescribed flow field is considered next. Steady state results for the dimensionless average heat flux from canister whose surface is at a constant temperature have been presented by Kimura [4] using a finite difference method. The results obtained in the present study using the finite element and the boundary-layer methods are compared with the published data in Table 1. The profile assumed in the boundary-layer method is, $T = (1-(r-1/\delta))^2$.

The comparison among the three solutions in Table 1 is seen to be good for the range $1 \leqslant Pe \leqslant 25$. It is to be noted that the boundary-layer approximations are not valid for $Pe < 1$, in transient and in array-interaction problems. The finite element solution is the only option available in such cases. Secondly the singularity of the boundary-layer equations as $\theta \to 0$ consistently predicts a higher heat transfer rate in Table 1 and a lower wall temperature and concentration in prescribed gradient problems.

Single canister. Heat and mass transfer from single canisters on the surface of which a prescribed heat flux or a leach rate for a single nuclide prevails is described below. See Table 2 for initial values of $\phi(\pi)$ for BLM and Table 3 for average concentration levels.

Numerical results show that the average concentration level given in Table 3 is nearly equal to the local maximum value on the canister surface for $Pe \leqslant 1$. For $Pe = 10$ the maximum value is larger by a factor of two.

Table 1. Average wall heat flux from an isothermal canister placed in flow

Pe	0.1	1	2.5	5	10	25	50	100
FEM	0.143	0.74	1.126	1.564	2.22	3.39	3.41	—
BLM	0.232	0.734	1.115	1.64	2.32	3.66	5.19	7.34
Kimura [4]	0.221	0.697	1.103	1.56	2.20	3.48	4.93	6.97

Table 2. Initial values of ϕ at $\theta = \pi$

	Pe		
b	1	10	100
0.1	2.8013	0.2839	0.02851
1	1.7989	0.1929	0.01977
10	0.4393	0.0478	0.00493

Canister array. We study below an array of five canisters using the finite element method. Average concentrations at steady state on the central canister are presented in Table 4. Two different values of the separation parameter, $d = 6$ and 8, have been considered in the present study.

The following observations can be made from Table 4. The results for $b = 0$ and $b = 0.1$ are quite close to each other and effects of decay are seen only for $b > 0.1$. This is consistent with the result obtained for a single canister (Table 3). Interaction effects lead to an increase in the average wall concentration. This is significant at low Peclet number ($Pe \leqslant 1$) and is virtually absent for $Pe \geqslant 10$. The presence of several canisters increases the local velocity in the gaps between them and can result in a slight lowering of the wall concentration. For spacing $d = 6$ and 8 this lowering is not significant even at $Pe = 10$.

Flow past canisters: Transient evolution

For a prescribed gradient condition on a canister surface the wall concentration reaches a maximum at steady state. The maximum value depends on the flow parameter Pe and the decay parameter b. It is important to know the time scale involved in reaching steady state. The porous formation is assumed to be initially cold in the temperature problem ($T(\mathbf{x}, 0) = 0$) and clean in the concentration problem ($c(\mathbf{x}, 0) = 0$). The flow itself is assumed to be steady in the present discussion. Figure 4 shows the increase in the average concentration on the surface of an isolated canister with time for different values of Pe and b. The result for $b = 0$ is close to that for $b = 0.1$ and is not shown. Figure 5 shows a similar plot for the central canister

Table 3. Average wall temperature/concentration on a canister with a prescribed heat flux

		Pe			
b		0.1	1.0	10.0	100.0
0	FEM	1.89	1.236	0.421	—
	BLM	—	1.59	0.503	0.159
0.1	FEM	1.8174	1.1033	0.3905	—
	BLM	—	1.447	0.47	0.15
1.0	FEM	1.42	0.68	0.228	—
	BLM	—	0.92	0.32	0.104
10.0	FEM	0.707	0.248	0.049	—
	BLM	—	0.36	0.12	0.038

Table 4. Average wall concentration on the central canister of an array

		Pe		
d	b	0.1	1.0	10.0
6	0	4.05	2.18	0.45
	0.1	3.81	1.71	0.42
	1.0	2.51	0.77	0.22
	10.0	0.79	0.24	0.044
8	0	2.83	1.75	0.46
	0.1	2.67	1.43	0.42
	1.0	1.84	0.71	0.23
	10.0	0.72	0.24	0.047

of an array that is shown in Fig. 1. The result for $Pe = 10$ is not plotted in Fig. 5 since it is identical to that shown in Fig. 4. The general trend seen in Figs. 4 and 5 is as follows. Steady state is attained faster at higher values of b. The short time solution for $t \leqslant 0.01$ is, however, nearly independent of b and depends only on the Peclet number. For both a single canister and an array steady state is reached for small values of b ($b \leqslant 0.1$) in a dimensionless time of 3 units independent of Pe. Since the time scale is U/R the dimensional time required to reach steady state is $3R/U$. This quantity decreases with increasing U and hence increasing values of Pe. For $R = 1$ m and $U = 10$ m yr^{-1} the time required to reach steady state is 30 yr. Safety analysis is usually carried out over a much longer time period and transients may be unimportant in such a study.

The reduction in the real time required to reach steady state with increasing b and Pe can be explained as follows. The steady state represents an equilibrium among the mechanisms of diffusion, advection and decay of a nuclide. At small time the extent of the affected region around a canister represented by the boundary-layer thickness δ is small. Since diffusion occurs across a concentration gradient a small δ leads to a large diffusive transport into the flow domain. Radioactive decay is distributed over the volume of the affected region and is small when δ is small. Hence at small time we have diffusion > convection + decay. As a consequence δ increases with time till diffusion effects reduce in magnitude and the amount of decay becomes significant. At steady state the left and right hand sides of the inequality given above are strictly equal. Clearly the equality is attained rapidly if Pe (convection) or b (decay) is increased. In a conduction heat transfer problem Pe and b are zero and no steady state is possible.

Parent–daughter model

Equation (4) describes transport of a pair of nuclides A and B which follow the reaction A → B. Here A is identified as a parent and B as a daughter. On decay A is completely converted to B and so the factor R_p in equation (2) is unity. In the waste disposal application B is usually more stable than A with a half

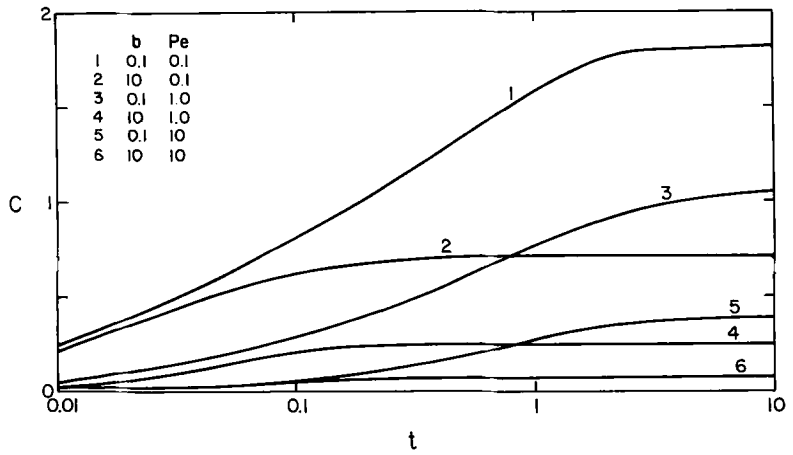

FIG. 4. Increase in wall concentration with time: effect of flow.

life at least two orders of magnitude larger than that of A. Hence the decay parameter b for the daughter nuclide is small and is set to zero in the present problem. The decay parameter in the discussion below refers to the parent alone. The following cases have been considered:

1. Diffusion limit.
2. Convective transport due to fluid flow.

At the diffusion limit the concentration level of a stable daughter is governed by the equation,

$$c_t = c_{rr} + \frac{1}{r}c_r + bc_A(r,t)$$

with the condition, $c(t=0) = 0$, $-c_r(r=1) = L_B$ and $c(r=\infty) = 0$. Here L_B is the leach rate of nuclide B and is 0 or 1; b is the decay parameter of the parent A. The analytical solution of this equation is,

$$c = L_B c_A + bc_B$$

where $c_A = c(r,t;\, b=0)$, the concentration level of nuclide A with b set to zero (equation (12)) and

$$c_B(r,t) = \int_0^\infty d\beta \frac{\beta R_0(\beta,r)R_0(\beta,1)F(\beta,t)}{(b+\beta^2)^2 N(\beta)}$$

where

$$F(\beta,t) = b(1-e^{-\beta^2 t}) - \beta^2 e^{-\beta^2 t}(1-e^{-bt}).$$

Since c_A increases monotonically with time the daughter concentration is also an unbounded function of time unless L_B is zero. When L_B is zero the nuclide B is produced in the porous region only by the decay of A and a steady state is possible. Figure 6 shows a plot of c_B as a function of time.

Parent and daughter concentrations on the canister in the presence of flow are considered next. When equal fluxes of A and B prevail on the canister surface the steady state concentration of B exceeds that of A owing to the decay reaction A → B. The initial value $\phi_B(\pi)$ required for integrating the boundary-layer equations is given in Table 5.

Values of the average concentration of nuclide B as a function of Pe and b, the decay parameter of nuclide A are given in Table 6. As before the FEM solution

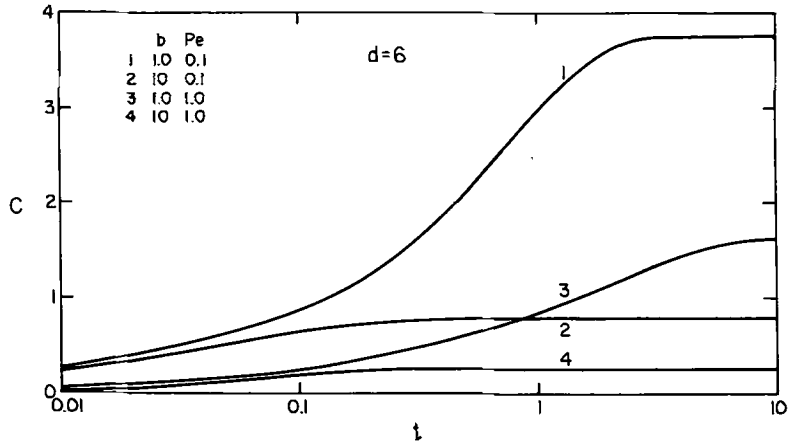

FIG. 5. Increase in wall concentration on the central canister of an array with time: effect of flow.

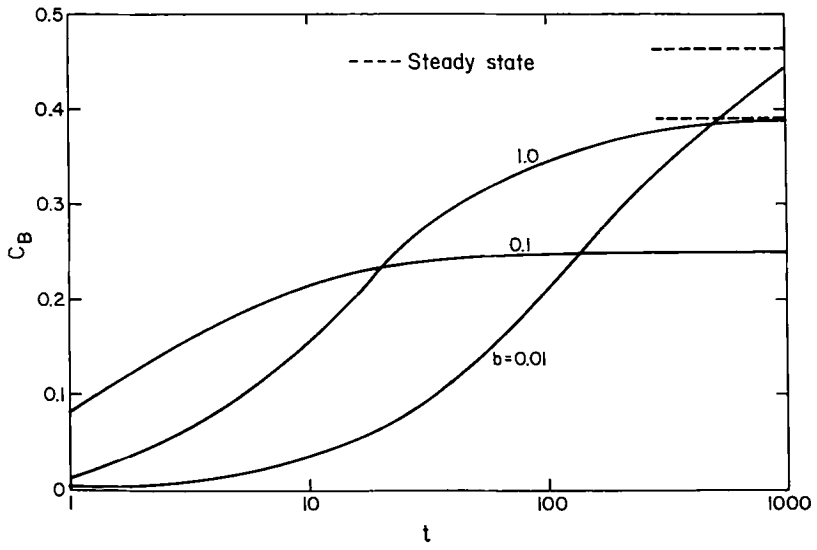

FIG. 6. Increase in function c_B with time in parent–daughter problem.

Table 5. Initial values of ϕ_B at $\theta = \pi$; boundary-layer solution

	Pe		
b	1	10	100
0.1	3.1986	0.3161	0.03148
1	4.201	0.4071	0.0402
10	5.5606	0.5521	0.0551

at $Pe = 100$ and the BLM solution at $Pe = 0.1$ are not given here.

The average concentration of the parent nuclide is given in Table 3. The daughter concentration at steady state is always larger than that of the parent. Besides, the following observations can be made. The average daughter concentration drops with increasing Peclet number as in the case of the parent. However, increasing values of b reduce the parent concentration but increase that of the daughter. The extent of this increase depends on the relative importance of diffusion and convection and hence the Peclet number. It is small at higher values of Pe. The daughter concentration is a stronger function of Pe than of b. For example as Pe changes from 1 to 10 the concentration drops by about a factor of three. When b changes from 1 to 10 the concentration increases by about 30%.

Results are given in Table 7 for the average daughter concentration when the prescribed fluxes of A and B on the canister surface are 1 and 0 respectively. Here the daughter nuclide is produced entirely by the decay of the parent. The former is assumed to be stable. The boundary-layer method with a quadratic profile is inapplicable here because it predicts a finite non-zero gradient at the wall. Calculations for this problem have been carried out using the finite element method.

Since nuclide B is produced entirely by the decay of A the daughter concentration at steady state is a strong function of the decay parameter b. It continues to depend strongly on Pe as well.

In comparison to the single nuclide problem the transients here are of a long duration and steady state is attained in about ten dimensionless units. Increasing b reduces the transient period for the parent nuclide but increases that of the daughter. When the latter is produced entirely due to the decay of the parent there is further delay in the build-up of the daughter concentration.

Table 6. Average concentration of the daughter nuclide

		Pe			
	b	0.1	1	10	100
FEM	0.1	3.58	1.38	0.46	—
BLM		—	1.746	0.541	0.169
FEM	1	4.65	1.805	0.625	—
BLM		—	2.052	0.638	0.20
FEM	10	5.45	2.24	0.80	—
BLM		—	2.242	0.71	0.224

Table 7. Average daughter concentration on canister surface

	Pe		
b	0.1	1	10
0.1	0.502	0.14	0.036
1	1.58	0.56	0.20
10	2.37	0.99	0.38

CONCLUSIONS

The following conclusions have been drawn in the present study.

The average concentration level of a nuclide on the surface of a canister decreases with increasing Peclet number Pe and the decay parameter b.

The average concentration reaches a maximum at steady state. When $Pe = b = 0$ no steady state exists and the maximum value is unbounded.

The real time required to reach steady state decreases with increasing values of Pe and b.

Canister interaction effects are important at steady state, small values of b ($\leqslant 1$) and small values of Pe ($\leqslant 1$).

For $Pe > 1$ the boundary-level method is a rapid way of determining concentration levels on single canisters at steady state.

REFERENCES

1. T. W. Broyd, Benchmark studies of computer prediction techniques for equilibrium chemistry and radionuclide transport in groundwater flow. In *Nuclear Containment* (Edited by D. G. Walton). Cambridge University Press, U.K. (1988).
2. P. S. Huyakorn, B. H. Lester and J. W. Mercer, An efficient finite element technique for modelling transport in fractured porous media ; Part 1, single species transport and Part 2, nuclide decay chain transport, *Water Resources Research* **19**(3), 841–854 and 1286–1296 (1983).
3. S. Kimura, Transient forced and natural convection heat transfer about a vertical cylinder in a porous medium, *Int. J. Heat Mass Transfer* **32**, 617–620 (1989).
4. S. Kimura, Transient forced convection heat transfer from a circular cylinder in a saturated porous media, *Int. J. Heat Mass Transfer* **32**, 192–195 (1989).
5. W. M. Kays and M. E. Crawford, *Convective Heat and Mass Transfer*. McGraw-Hill, New York (1980).
6. J. Bear, *Dynamics of Fluids in Porous Media*. Elsevier, New York (1979).
7. A. J. Baker, *Finite Element Computational Fluid Mechanics*. McGraw-Hill, New York (1983).
8. I. S. Duff, MA 28—A set of fortran subroutines for sparse unsymmetric linear equations, AERE Harwell (1980).
9. K. Muralidhar, Flow and transport in single rock fractures, J. Fluid Mechanics **215**, 481–502 (1990).